Carbohydrate Polymers 89 (2012) 948–954

Contents lists available at SciVerse ScienceDirect

Carbohydrate Polymers

journal homepage: www.elsevier.com/locate/carbpol

Peptide-functionalized chitosan–DNA nanoparticles for cellular targeting

Elina Talvitie[a,c,*], Jenni Leppiniemi[b,c], Andrey Mikhailov[d], Vesa P. Hytönen[b,c,e], Minna Kellomäki[a,c]

[a] Department of Biomedical Engineering, Tampere University of Technology, FI-33101 Tampere, Finland
[b] Institute of Biomedical Technology, University of Tampere and Tampere University Hospital, FI-33014 University of Tampere, Finland
[c] BioMediTech, FI-33520 Tampere, Finland
[d] Department of Otolaryngology, University of Tampere and Tampere University Hospital, FI-33014 University of Tampere, Finland
[e] Center for Laboratory Medicine, Tampere University Hospital, FI-33520 Tampere, Finland

ARTICLE INFO

Article history:
Received 29 February 2012
Received in revised form 10 April 2012
Accepted 12 April 2012
Available online 21 April 2012

Keywords:
Chitosan
Nanoparticle
Gene delivery
Targeting

ABSTRACT

Chitosan–pDNA nanoparticles with various weight ratios (chitosan:pDNA 1:4–8:1) were characterized for particle size, zeta potential, morphology, and pDNA binding efficiency. For targeted gene delivery applications, nanoparticles were functionalized by coupling fluorescent dye and tyrosine kinase receptor B (TrkB) binding peptides on the particle surface. The targetability of the peptide-functionalized nanoparticles was demonstrated in TrkB positive murine transformed monocyte/macrophage cells (RAW 264). It was observed that weight ratio influenced DNA condensation and nanoparticle properties. An increase in the weight ratio decreased the average particle size, but increased the zeta potential. Cell culture studies showed that TrkB-peptide-functionalized nanoparticles bound to cells more effectively than nanoparticles functionalized with a control peptide. The length of the PEG spacer arm of the amine-to-sulfhydryl crosslinker used in the functionalization was found to positively correlate with the cellular attachment efficiency. This study suggests that the peptide-functionalization could be used to target chitosan–pDNA nanoparticles to specific cells.

1. Introduction

Cationic polymers and liposomes have been extensively studied as potential DNA carriers for non-viral gene delivery. Cationic polymers are positively charged and interact electrostatically with anionic DNA. These electrostatic interactions between polymer and DNA result in the formation of polymer–DNA complexes or nanoparticles (Opanasopit, Rojanarata, Apirakaramwong, Ngawhirunpat, & Ruktanonchai, 2009). Various cationic polymers such as polyethylenimine (PEI) (Ahn et al., 2008; Kunath et al., 2003; Wightman et al., 2001), poly-L-lysine (PLL) (Carlisle, Read, Wolfert, & Seymour, 1999; Mann, Richa, & Ganguli, 2008), polyamidoamine dendrimers (Navarro & Tros de ILarduya, 2009; Peng et al., 2010), and chitosan (Leong et al., 1998; Richardson, Kolbe, & Duncan, 1999) have all been reported to be able to condense DNA and have been used as gene carriers.

Non-viral carriers have several advantages when compared with unsafe viral vectors (retrovirus, adenovirus, adeno-associated viruses, herpes simplex virus, and lentivirus) (Corsi, Chellat, Yahia, & Fernandes, 2003). The non-viral systems can be tailored to target specific cells or tissues and they elicit only low host immune response. The non-viral systems provide an advantage in long-term storage, and they can also be produced in large volumes and at reasonable cost (Corsi et al., 2003; Mao et al., 2001). In gene delivery applications, the balance between stability and instability, the capability to protect DNA from nuclease degradation, targetability, and biocompatibility are important characteristics of efficient polymer–DNA complexes and nanoparticles (Mao et al., 2001).

Chitosan is a linear polymer composed of randomly repeating *N*-acetyl-D-glucosamines and D-glucosamines. Chitosan is obtained by alkaline deacetylation from chitin that is a natural polysaccharide found in the exoskeleton of crustaceans and insects and also in the cell walls of certain fungi (Muzzarelli et al., 2012). Chitosan has amino groups with a pK_a value of approximately 6.5. Thus, chitosan is positively charged and interacts with anionic DNA at acidic pH to form chitosan–DNA nanoparticles (Jayakumar et al., 2010). The molecular weight, degree of deacetylation, and the weight or charge ratio of chitosan to DNA has been shown to influence the properties of the chitosan–DNA delivery systems and their transfection efficiency (Huang, Fong, Khor, & Lim, 2005; Kiang, Wen, Lim, & Leong, 2004; Lavertu, Méthot, Tran-Khanh, & Buschmann, 2006; Strand et al., 2010). Conditions of nanoparticle synthesis such

Abbreviations: NHS, *N*-hydroxysuccinimide; PEG, polyethylene glycol; MAL, maleimide; TrkB, tyrosine kinase receptor B; RAW 264, murine transformed monocyte/macrophage cell line; PDI, polydispersity index; PEP, peptide; cPEP, control peptide.

* Corresponding author at: Department of Biomedical Engineering, Tampere University of Technology, FI-33101 Tampere, Finland. Tel.: +358 40 849 0976; fax: +358 3 3115 2250.
E-mail address: elina.talvitie@tut.fi (E. Talvitie).

0144-8617/$ – see front matter © 2012 Elsevier Ltd. All rights reserved.
http://dx.doi.org/10.1016/j.carbpol.2012.04.042

as the concentration of chitosan and DNA, ionic strength, and pH also influence chitosan–DNA particle properties like size and shape (Köping-Höggård, Mel'nikova, Vårum, Lindman, & Artursson, 2003; Mao et al., 2001; Romøren, Pedersen, Smistad, Evensen, & Thu, 2003). In addition to its cationic nature, chitosan is a biodegradable, biocompatible, and non-toxic material (Muzzarelli, 2010). Because of its favorable characteristics, chitosan is also studied in oral, nasal, and ocular drug delivery applications (Amidi et al., 2006; De Campos, Sánchez, & Alonso, 2001; Trapani et al., 2010; van der Lubben, Verhoef, van Aelst, Borchard, & Junginger, 2001; Yuan, Li, & Yuan, 2006).

Targeted delivery systems are essential for efficient and safe gene or drug delivery. Targetable nanoparticles can be achieved by conjugating targeting ligands such as small molecules, peptides, and proteins on the nanoparticle surface (Davis, 2002). Ligands enable the binding of the nanoparticles to specific target receptors on cells and internalization through various mechanisms. Functionalization of the nanoparticle surface does not only improve targetability but may also enhance cellular uptake, thereby making the gene transfer more efficient (Mao et al., 2001).

Some studies on chitosan–DNA delivery systems targeted to specific receptors have been reported. In these studies, nanoparticles were functionalized by conjugating transferrin (Mao et al., 2001), KNOB protein (Mao et al., 2001), and endosomolytic peptides GM225.1 and GM227.3 (MacLaughlin et al., 1998) to the nanoparticle surface. To improve nuclear uptake, delivery systems containing nuclear localization signal (NLS) peptides that attach to cytoplasmic transport receptors, have been investigated (Opanasopit et al., 2009). In addition, non-proteinaceous ligands such as folate (Chan, Kurisawa, Chung, & Yang, 2007; Mansouri et al., 2006) and hyaluronic acid (de la Fuente, Seijo, & Alonso, 2008) have been studied for targeting. Lactose (Hashimoto, Morimoto, Saimoto, Shigemasa, & Sato, 2006a), galactose (Gao et al., 2003; Kim, Park, Nah, Choi, & Cho, 2004), and mannose (Hashimoto et al., 2006b; Kim, Jin, Kim, Cho, & Cho, 2006) have been used as non-proteinaceous ligands in the production of chitosan derivatives for targeted gene delivery.

Brain-derived neurotrophic factor (BDNF) is a protein belonging to neurotrophins, i.e. a group of nerve growth factors that support the growth, differentiation, and survival of neuronal cells. Two neurotrophin receptors to which BDNF is able to bind exist on the cell surface: the low-affinity neurotrophin receptor p75 and the high-affinity receptor TrkB (García-Suárez et al., 1998; Ma et al., 2003). Therapeutic use of BDNF, e.g. in the treatment of neurodegenerative diseases is, however, restricted because of its molecular size, short half-life, and side effects. As a result, low molecular weight TrkB binding peptides have been developed (Ma et al., 2003) in order to mimic the actions of BDNF.

The aim of this study was to examine the functionalization of chitosan–pDNA nanoparticles by attaching TrkB binding targeting peptides and fluorescent dye on a nanoparticle surface. The conjugation of peptides was studied using crosslinkers with variable PEG spacer arm lengths. In addition, the effects of chitosan:pDNA weight ratio and surface modification on nanoparticle properties such as particle size and zeta potential were determined. To evaluate the binding of the nanoparticles to the cells, the peptide-functionalized chitosan–pDNA nanoparticles were studied in TrkB positive RAW 264 (murine transformed monocyte/macrophage) cells.

2. Materials and methods

2.1. Materials

Ultrapure chitosan PROTASAN UP B 80/20 with a molecular weight of 250 kDa and degree of deacetylation of 86% was purchased from FMC BioPolymer/NovaMatrix (Sandvika, Norway). Fluorescent dye DyLight 405 NHS ester as well as succinimidyl-([*N*-maleimidopropionamido]-#ethyleneglycol) ester (NHS-PEG$_n$-MAL) were purchased from Thermo Scientific (Rockford, IL, USA). Plasmid Id2.3 encoding green fluorescent protein (GFP) was obtained from Promega Corp. (Madison, WI, USA). GeneRuler^{TM} 1 kb DNA ladder, 6× DNA loading dye solution, and restriction enzyme PstI were from Fermentas (St. Leon-Rot, Germany). SYBR® Safe DNA gel stain was purchased from Invitrogen (Carlsbad, CA, USA). Other reagents were commercially available, higher-grade chemicals.

2.2. Peptide design and synthesis

Peptides were designed in a rational way on the basis of published TrkB binding sequences (Ma et al., 2003) and by inserting the sequence of the cleavage site for TeV protease between the N-terminal cysteine and the TrkB binding sequence. Peptide PEP (CENLYFQSG**SMAHPYFAR**) was used as a targeting peptide. Peptide cPEP (CENLYFQSGAYHMSAPFR) is a scrambled version of PEP with a randomized receptor-binding sequence. The recognition sequence for TeV protease is presented underlined and the TrkB binding sequence is presented in bold text. Both peptides have 18 amino acids and positive charge. All peptides were synthesized with FMOC technology at Storkbio (Tallinn, Estonia) and their purity (>90%) was verified by high performance liquid chromatography (HPLC) and their identity confirmed by mass spectrometry.

2.3. Cell culture

RAW 264 cell line was obtained from a local cryodepository and is descent from the original cells purchased from ATCC (Manassas, USA; clones TIB-71^{TM}) with less than 5 passages. The cells were maintained in Iscove's media supplemented with 5% fetal calf serum (Sigma, St. Louis, MO, USA) without any other nutritional supplements or antibiotics. The RAW 264 cells were maintained at a confluency lower than 50% in a humidified atmosphere at 5% CO_2.

2.4. Preparation of chitosan–pDNA nanoparticles

Chitosan nanoparticles loaded with plasmid DNA (pDNA) were prepared using complex coacervation. First, chitosan was dissolved in 100 mM acetic acid, 100 mM sodium acetate buffer overnight. Then, the pH of the chitosan solutions was adjusted to 5.5 with 10 M NaOH and the solutions were passed through a 0.2 μm syringe filter before use. Plasmid DNA was diluted in a 5 mM sodium sulfate solution. The chitosan and pDNA solutions were heated separately to 55 °C, followed by the immediate addition of the plasmid solution into the chitosan solution. The temperature of the solutions affects the size of the forming nanoparticles. At 55 °C using chitosan concentration of 50–400 μg/ml and DNA concentration of 40–80 μg/ml, uniform nanoparticles have been obtained (Mao et al., 2001). Finally, the mixture was vortexed for 30 s and then incubated at room temperature (RT, 22 ± 1 °C) for 30 min to complete the nanoparticle formation. The following chitosan to pDNA weight ratios were used: 1:4, 1:2, 1:1, 2:1, 4:1, and 8:1.

2.5. Functionalization of chitosan–pDNA nanoparticles

Targeting peptides and a fluorescent dye were coupled to amines at the surface of a nanoparticle after particle formation. The conjugation of the peptides was a two-step reaction, in which an amine-to-sulfhydryl crosslinker with polyethylene glycol (PEG) spacer arms, NHS-PEG$_n$-MAL, was used (Fig. 1). Three different crosslinkers with varying PEG spacer arm lengths and molecular

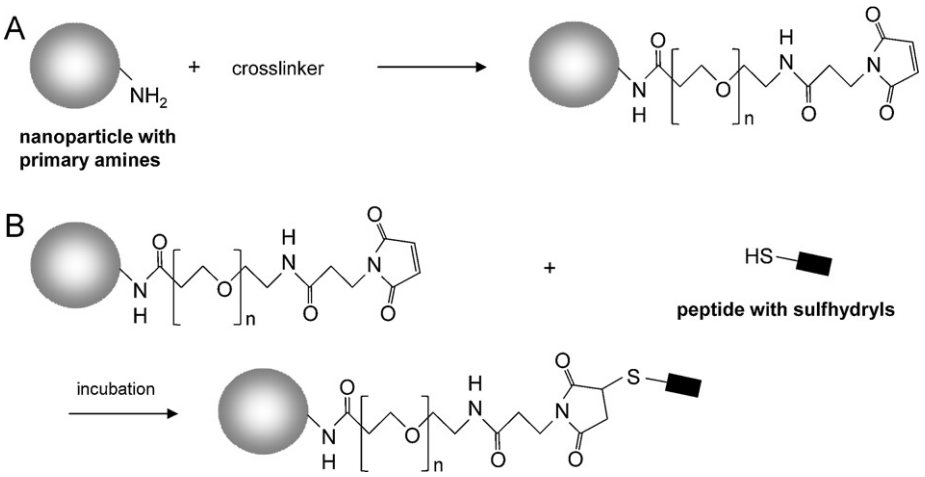

Fig. 1. Scheme for coupling a peptide to the surface of chitosan–pDNA nanoparticles using a heterobifunctional crosslinker with PEG spacer arms. (A) Coupling of NHS-PEG$_n$-MAL to the amines at the nanoparticle surface. (B) Reaction between NHS-PEG$_n$-MAL and peptide with N-terminal cysteine.

weights were studied: PEG_2 (17.6 Å, 425.39 g/mol), PEG_6 (32.5 Å, 601.60 g/mol), and PEG_{12} (53.4 Å, 865.92 g/mol).

To provide applicable conditions for the conjugation processes, the pH of the nanoparticle solution was increased to 7.0–7.2 by adding PBS buffer (100 mM sodium phosphate, 100 mM sodium chloride, pH 8). A 50-fold molar excess of crosslinker and a 16-fold molar excess of fluorescent dye to chitosan were mixed with the nanoparticle solution and incubated at RT for 1 h. Then, a 50-fold molar excess of peptide to chitosan was added into the nanoparticle solution and the incubation was continued at RT for 30 min. Non-reactive reagents and by-products were removed by dialysis in PBS buffer (50 mM sodium phosphate, 100 mM sodium chloride, pH 5.3) using a dialysis membrane with a molecular weight cut-off of 12,000–14,000 Da. The dialyzed nanoparticle solutions were stored at 4 °C.

2.6. Characterization of chitosan–pDNA nanoparticles

2.6.1. Particle size, polydispersity index, and zeta potential

A dynamic light scattering (DLS) instrument Zetasizer Nano ZS (Malvern Instruments Ltd., Worcestershire, UK) was used to determine the hydrodynamic diameter of the nanoparticles. The measurements were carried out at 25 °C using a scattering angle of 173°. Each sample was measured twice with three parallel measurements using a disposable sizing cuvette. The polydispersity index (PDI) was recorded for each nanoparticle as a measure of particle size distribution.

The zeta potential was defined by laser Doppler velocimetry (LDV) using the Zetasizer Nano ZS with Smoluchowski as a measurement model. The measurements were performed at 25 °C in disposable folded capillary cells. Each sample was measured three times.

2.6.2. Morphology

Morphology was studied using field emission scanning electron microscopy (FE-SEM, Zeiss ULTRA plus, Carl Zeiss NTS GmbH, Oberkochen, Germany). The samples were prepared for FE-SEM by pipetting a small amount of the nanoparticle solution onto a copper grid and incubating the solution for a few minutes. A filter paper was used to remove the excess nanoparticle solution. Before sample preparation, the nanoparticle solutions were dialyzed in PBS buffer (pH 5.3) or sterile water. Both carbon-coated and non-coated FE-SEM samples were examined.

2.6.3. Agarose gel electrophoresis

The capacity of chitosan to bind with pDNA was evaluated using agarose gel electrophoresis. Naked pDNA and nanoparticles with different chitosan to pDNA weight ratios (1:4, 1:2, 1:1, 2:1, 4:1, and 8:1) were studied. Samples mixed with a loading dye were loaded to a 0.8% agarose gel in Tris–borate EDTA (TBE) buffer, and run at 80 V (400 mA) for 1 h. The gel was prestained with SYBR® Safe DNA gel stain and visualized under UV light using a Bio-Rad ChemiDoc™ XRS molecular imager (Bio-Rad Laboratories, Inc., Hercules, CA, USA).

To study the protection effect of the nanoparticles to plasmid, PstI restriction enzyme was selected to cut the plasmid in two fragments. The following three samples were digested with PstI: the naked pDNA and the nanoparticles with the chitosan to pDNA weight ratios of 1:4 and 4:1. PstI was pipetted into a solution consisting of a digested sample, sterile water, and 10× buffer O. The mixture was incubated at 37 °C for 1 h and the reaction was stopped by adding 0.5 M EDTA (pH 8) to achieve a final concentration of 20 mM. After digestion, the samples were analyzed by gel electrophoresis as described above.

2.7. Cell culture studies

Estimation of binding efficiency was performed on a suspension of EDTA-detached RAW 264 cells naturally expressing the TrkB receptor. The peptide-bearing nanoparticles were added to the suspension of the cells at 1:5000 dilution with 10^6 cells per sample, incubated for 1, 6, or 22 h at room temperature in 5 mM Hepes containing 135 mM NaCl (pH 7.4), washed four times with PBS and then fixed in 4% paraformaldehyde in PBS. The fixed cells were measured using a Becton Dickenson FACSAria flow cytometer (BD Biosciences, Franklin Lakes, NJ, USA).

To distinguish whether the particles were bound to the receptors or internalized inside the cells, 100 E/ml of TeV protease was added to the cells before the addition of the nanoparticles. The cells were treated and analyzed as described above. Because the nanoparticles are supposed to bind to the cell surface via affinity interaction between the peptide and TrkB receptors, they should be released by the TeV protease that cleaves the peptide sequence between the nanoparticle and the recognition sequence of TrkB. Once the particles are internalized, however, the TeV treatment should not affect the fluorescence signal from the nanoparticles.

3. Results and discussion

3.1. Particle size, polydispersity index, and zeta potential

The chitosan–pDNA nanoparticles were formed by electrostatic interactions between chitosan and DNA. The electrostatic

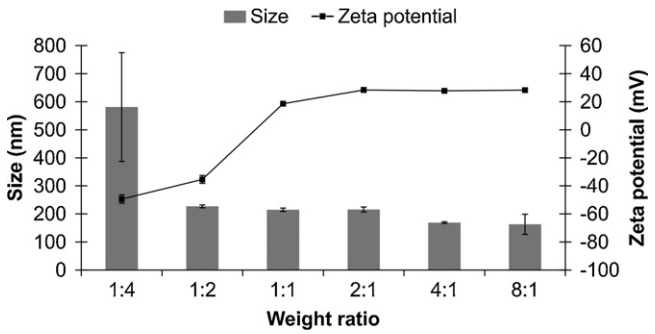

Fig. 2. Size (average hydrodynamic diameter) and zeta potential of nanoparticles prepared using different chitosan to pDNA weight ratios (w:w). The error bars represent the standard deviation.

interactions between the positively charged chitosan and negatively charged DNA resulted in phase separation (polymer-rich phase and polymer-poor phase) when these oppositely charged polyelectrolytes were mixed in an aqueous solution. The phase separation and coacervate formation was enhanced by using sodium sulfate as a coacervation agent (Leong et al., 1998).

The average hydrodynamic diameters for the chitosan–pDNA nanoparticles having different chitosan to pDNA weight ratios varied from 163 ± 36 nm to 581 ± 194 nm. The highest average diameter was obtained for the nanoparticles having the lowest chitosan to pDNA weight ratio. As shown in Table 1 and Fig. 2, the hydrodynamic diameter clearly showed a negative correlation with weight ratio.

Polydispersity indexes were elevated at low and high weight ratios (Table 1). The size distribution became bimodal at high weight ratio (w:w, 8:1), as smaller and larger particle populations were detected (peaks at 33 ± 3 nm, 190 ± 61 nm). This may indicate that the nanoparticles are aggregating or there are free molecules present in the sample. Monomodal particle size distributions were obtained at lower weight ratios. However, the weight ratio of 1:4 resulted in a remarkable particle size increase showing also high PDI and multimodal size distribution (two major peaks at 18 ± 2 nm and 662 ± 272 nm). The particle size distributions by volume are listed in Table 1 that shows the monomodal or multimodal size distributions.

The zeta potential of the nanoparticles varied from −49 mV to +28 mV (Table 1 and Fig. 2, measured at pH ~ 5.5). Zeta potentials of −49 mV and −35 mV were measured for the nanoparticles with weight ratios of 1:4 and 1:2, respectively. These results may indicate that there was an excess of pDNA in the mixture and that the binding of pDNA to chitosan was incomplete resulting in highly negative zeta potential. At weight ratios from 2:1 to 8:1, zeta potential remained at the level of approximately +28 mV showing condensation of pDNA and the formation of nanoparticles with free amines at the surfaces. Other studies have also shown similar changes in particle size and zeta potential when the charge ratio of the chitosan–DNA complexes was changed (Erbacher, Zou, Bettinger, Steffan, & Remy, 1998; Kim et al., 2004). Thus, weight or charge ratio has an evident connection to particle size and zeta potential.

3.2. Morphology

According to the FE-SEM studies, the morphology of the chitosan–pDNA nanoparticles seemed to be spherical. Aggregating nanoparticles were also observed, corresponding to the obtained DLS results. At the weight ratio of 4:1, the nanoparticles aggregated only slightly (Fig. 3A). However, aggregation was more obvious at the weight ratio of 8:1 (Fig. 3B). The size of the nanoparticles

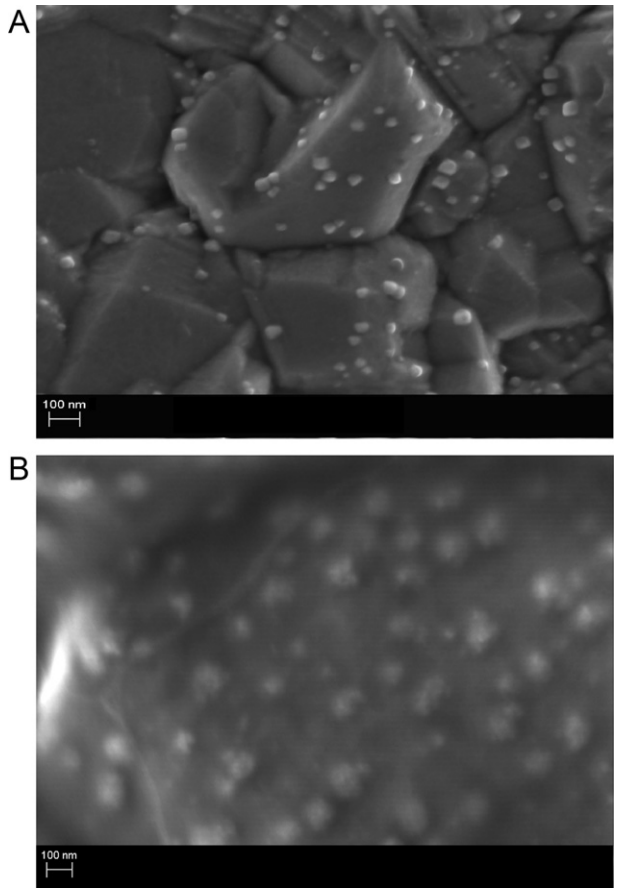

Fig. 3. Morphology of chitosan–pDNA nanoparticles studied by FE-SEM. Chitosan to pDNA weight ratio (A) 4:1 and (B) 8:1. Scale bar 100 nm.

(w:w, 4:1) estimated by FE-SEM analysis was approximately 40 nm, while according to the DLS measurement the size was 169 nm. In DLS analysis, the particle size was measured from the aqueous nanoparticle suspensions and chitosan has a tendency to swell when in contact with water. In contrast, the samples were dried for the FE-SEM studies, and this may explain the differences between the FE-SEM and DLS results (Aktas et al., 2005). Analogously, DNA requires water to form a natural helical conformation that collapses when dried (Dickerson et al., 1982).

Charge ratio has been reported to affect the shape of the chitosan–pDNA complexes. Liu et al. observed aggregates and irregular complexes at low charge ratio, but spherical complexes at higher charge ratios. They concluded that at high charge ratio chitosan is able to condense DNA completely to form spherical complexes (Liu et al., 2005). In addition, toroidal and rod-like structures have been observed (Danielsen, Vårum, & Stokke, 2004; Erbacher et al., 1998).

3.3. DNA binding capability

The capacity of the chitosan and pDNA to form nanoparticles together was evaluated by agarose gel electrophoresis. The naked plasmid migrated on the gel (Fig. 4, lane 2), whereas DNA loaded into the chitosan nanoparticles with weight ratio 1:1–8:1 (lanes from 5 to 8) was unable to migrate and remained in the gel loading wells, suggesting strong interaction between chitosan and DNA. At the weight ratios of 1:4 and 1:2, some plasmid was migrating freely on the gel (lanes 3 and 4). This was evidence that not all pDNA was tightly engaged by chitosan. In conclusion, it can be assumed that at the weight ratio of higher than 1:2, DNA was completely

Table 1
DLS analysis of particles. Average hydrodynamic diameter by volume, the distribution of hydrodynamic diameter by volume, the polydispersity index (PDI), and the zeta potential of non-functionalized and functionalized chitosan–pDNA nanoparticles at different chitosan to pDNA weight ratios (w:w).

Sample	Average diameter (nm)	Distribution of diameter by volume (nm). Percentual amount is indicated in parenthesis[a]		PDI	Zeta potential (mV)
w:w, 1:4	581 ± 194	18 ± 2 (6%)	662 ± 272 (91%)	0.362 ± 0.097	−49.4 ± 3.0[b]
w:w, 1:2	227 ± 5	227 ± 5 (100%)		0.139 ± 0.008	−35.4 ± 2.8[b]
w:w, 1:1	215 ± 6	215 ± 6 (100%)		0.107 ± 0.017	+18.6 ± 0.7[b]
w:w, 2:1	216 ± 9	216 ± 9 (100%)		0.187 ± 0.011	+28.4 ± 1.7[b]
w:w, 4:1	169 ± 3	169 ± 3 (100%)		0.188 ± 0.012	+27.8 ± 1.1[b]
w:w, 8:1	163 ± 36	33 ± 3 (11%)	190 ± 61 (89%)	0.248 ± 0.017	+28.3 ± 0.9[b]
Functionalized					
w:w, 4:1; blank	166 ± 3	166 ± 3 (100%)		0.215 ± 0.004	+19.6 ± 1.3[c]
w:w, 4:1; PEG_2		173 ± 6 (40%)	5000 ± 390 (60%)	0.259 ± 0.040	+18.9 ± 1.4[c]
w:w, 4:1; PEG_6		159 ± 13 (49%)	4740 ± 1050 (51%)	0.285 ± 0.053	+19.8 ± 1.6[c]
w:w, 4:1; PEG_{12}		193 ± 13 (44%)	4860 ± 540 (53%)	0.275 ± 0.058	+17.5 ± 0.8[c]

[a] Size distributions containing <5% of total are not shown.
[b] Particle solution, pH ~ 5.5.
[c] Nanoparticles in dialysis buffer, pH 5.3.

coupled with chitosan and remained in the loading well. Similar findings have been made earlier and suggest that the interaction between chitosan and pDNA become more effective when weight or charge ratio increases (Xu, Capito, & Spector, 2008; Zheng et al., 2007). Kiang et al. reported the influence of molecular weight and degree of deacetylation on the capability of chitosan to bind DNA. According to their study, chitosans with lower molecular weight or degree of deacetylation require a higher charge ratio to condense DNA completely (Kiang et al., 2004).

When pDNA and two samples of the chitosan nanoparticles were digested with restriction enzyme PstI, plasmid was cut into two fragments, 4120 bp and 1197 bp. The nanoparticles containing an excess amount of plasmid (w:w, 1:4) released most of the DNA (Fig. 4, lane 10). This demonstrated that at weight ratio of 1:4 plasmid was partly located on the nanoparticle surface or remained unbound and free in the solution and, therefore, exposed to enzymatic digestion with PstI. Nevertheless, part of the plasmid remained in the well with chitosan. In the case of the nanoparticles containing an excess amount of chitosan (w:w, 4:1), no released DNA was seen after PstI digestion. Therefore, at weight ratio of 4:1 plasmid was most probably located mainly inside the particle and chitosan protected it from digestion. These findings are in line with the zeta potential results.

3.4. Functionalization of chitosan–pDNA nanoparticles

The nanoparticles with chitosan to pDNA weight ratio 4:1, having the initial particle size of 169 nm, were selected for the functionalization studies because they were able to bind pDNA completely according to agarose gel electrophoresis and that they had the monomodal particle size distribution. The functionalization potential of these nanoparticles was studied by conjugating fluorescent dye DyLight 405 NHS ester and NHS-PEG_n-MAL crosslinkers of different sizes to amine groups of chitosan. This was followed by the conjugation of sulfhydryl-containing peptide (PEP, cPEP) to the maleimide group of crosslinker.

The used heterobifunctional crosslinker had two different reactive groups, NHS (*N*-hydroxysuccinimide) ester and maleimide group. NHS esters react with amines forming covalent amide bonds and releasing *N*-hydroxysuccinimide. In the two-step conjugation procedure NHS ester reaction is followed by maleimide reaction. Maleimides are sulfhydryl-reactive, and the double bond of maleimide may undergo a specific alkylation reaction with sulfhydryl group to form a stable thioether bond (Hermanson, 1996; Mattson et al., 1993).

As expected, surface modification increased the particle size. After coupling with DyLight 405, PEG crosslinker, and peptide, the size of the particles varied from 159 ± 13 to 193 ± 13 nm (Table 1). In addition, the functionalization seemed to partly induce the aggregation process since large aggregates with diameter ~5 μm appeared in all functionalized particles (Fig. 5). If these aggregates are excluded from the data analysis, the hydrodynamic diameter of the particles was 173 ± 6 nm with the shortest PEG_2 spacer arm and 159 ± 13 nm with the PEG_6 spacer arm. By contrast, the nanoparticles functionalized with the longest PEG spacer arm (PEG_{12}) were slightly larger with the average diameter of 193 ± 13 nm. MacLaughlin et al. have studied the effect of non-covalently attached pH-sensitive endosomolytic peptides on the complex size and zeta potential. The size of the complexes

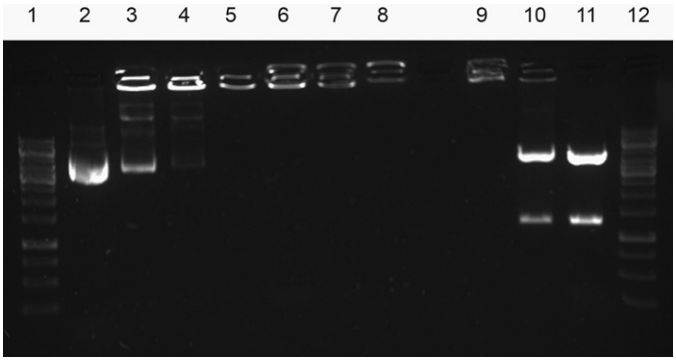

Fig. 4. Agarose gel electrophoresis of chitosan–pDNA nanoparticles having different chitosan to pDNA weight ratios (w:w). Lane 1: DNA ladder; lane 2: naked plasmid; lane 3: w:w, 1:4; lane 4: w:w, 1:2; lane 5: w:w, 1:1; lane 6: w:w, 2:1; lane 7: w:w, 4:1; lane 8: w:w, 8:1; lane 9: digested w:w, 4:1; lane 10: digested w:w, 1:4; lane 11: digested plasmid; and lane 12: DNA ladder.

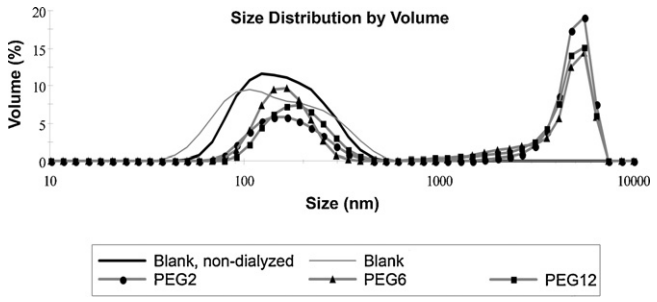

Fig. 5. Particle size distribution by volume of chitosan–pDNA nanoparticles functionalized with fluorescent dye DyLight 405 and different crosslinkers conjugated with peptide PEP. Nanoparticles without any functionalization (blank) were used as a control.

Table 2
Fluorescence of cells incubated for 1, 6, and 22 h with chitosan–pDNA nanoparticles. As a control measurement, the fluorescence of cells incubated for 22 h in the presence of TeV protease is shown. The results are indicated as mean*10^3 ± CV*10^3.

Incubation time	PEG_2		PEG_6		PEG_{12}	
	PEP	cPEP	PEP	cPEP	PEP	cPEP
1 h	7.5 ± 0.1	3.7 ± 0.2	8.0 ± 0.1	1.7 ± 0.1	9.2 ± 0.1	2.9 ± 0.3
6 h	10.4 ± 0.1	5.0 ± 0.3	12.7 ± 0.1	3.3 ± 0.3	10.8 ± 0.1	4.2 ± 0.3
22 h	19.3 ± 0.1	9.5 ± 0.2	21.6 ± 0.1	17.0 ± 0.3	22.9 ± 0.1	6.9 ± 0.3
22 h TeV protease	15.2 ± 0.1	6.6 ± 0.2	17.1 ± 0.1	12.4 ± 0.3	20.6 ± 0.1	5.7 ± 0.3

increased with increasing peptide amount. However, at higher peptide proportions (charge ratio of plasmid to peptide 1:1.5) the complex size decreased (MacLaughlin et al., 1998). Studies of the chitosan–DNA complexes functionalized with NLS peptides showed that at high chitosan to DNA weight ratios (8:1 and higher) the particle size was smaller compared with the complexes without NLS peptide. At lower weight ratios the particle size increased when NLS was added (Opanasopit et al., 2009).

The zeta potential of the peptide-functionalized nanoparticles varied between +18 and +20 mV (Table 1, measured at pH 5.3). These values are almost equal to the zeta potential of the dialyzed blank nanoparticles, +20 mV, indicating that this functionalization does not change the zeta potential of the particles. However, as the particles are more stable when the zeta potential is highly negative (<−30 mV) or highly positive (>+30 mV), we can conclude that the functionalized and even our dialyzed blank nanoparticles have a tendency to aggregate. Interestingly, the zeta potential of the non-dialyzed, blank nanoparticle was higher, +28 mV, at pH 5.5 indicating that they were more stable before dialysis. An increase in the number of surface peptides has been reported to diminish the zeta potential of the complexes containing endosomolytic peptides (MacLaughlin et al., 1998).

3.5. Cell culture studies

Targeting ligands enable ligand conjugated nanoparticles to be transported to the target cells by binding to the receptors on the cell surface. Our results demonstrate that the decoration of the chitosan–pDNA nanoparticles with affinity peptide (PEP) against TrkB significantly increased the binding of these nanoparticles to their target cells in the time-dependent manner. Table 2 illustrates the fluorescence of the cells after 1, 6, and 22 h incubation with the peptide-functionalized nanoparticles. FACS studies also showed that the longer PEG spacer arm was beneficial for TrkB binding. Clearly less efficient binding was seen with scrambled control peptide (cPEP). It is noticeable that the longer spacer gives higher specificity between targeting and scrambled peptides, as well as higher absolute binding of the nanoparticles. This behavior could be explained by the lower sterical hindrance of the peptides attached to the longer spacer, as well as the higher hydrophilicity of the longer PEG spacer reducing unspecific binding by van der Waals interaction.

Pretreatment with TeV protease specifically removes affinity peptides from the termini of the PEG spacer. As expected, the TeV treated samples demonstrated a lower fluorescence signal in all experimental groups (Table 2). However, the TeV treated functionalized particles still showed more binding compared with the particles decorated with the scrambled peptide, possibly suggesting either fast nanoparticle internalization or incomplete cleavage of the peptides by TeV. Our data show that the treatment of the affinity peptide-bearing nanoparticles with TeV protease partially reverses the effects of peptides on the binding and internalization of the particles. However, in our earlier studies (results not shown), we noticed that when TeV protease was added after 1 or 12 h incubation, fluorescence was higher compared with the samples pretreated with TeV. This proposes the fast dynamics of the steps critical for internalization. Finally, we propose that the measured fluorescence in the presence of TeV protease was obtained from the internalized nanoparticles, and that cell uptake was enhanced when the length of PEG spacer arm was increased.

4. Conclusions

Nanoparticles can be used in gene delivery as efficient and protective carriers for DNA. Targeting enables the delivery of therapeutic agents to the specific, predetermined cells. In targeted delivery, the availability of the delivered therapeutic agent can be improved and, hence nonspecific delivery can be avoided. This reduces unwanted effects and also decreases the amount of materials needed for efficient treatment.

Chitosan–pDNA nanoparticles with various chitosan to pDNA weight ratios were prepared, and the properties of the nanoparticles were affected by the weight ratio. Targeting peptides were successfully coupled on the nanoparticle surface, and surface modification only slightly reflected to the particle properties. The functionalization of the nanoparticles with TrkB binding affinity peptide was shown to enhance the binding to the cells having TrkB receptors in a specific and time-dependent manner. The PEG spacer arm length of the NHS-PEG_n-MAL crosslinker was found to positively correlate with the binding efficiency.

Acknowledgments

This study was financially supported by the European Community 6th Framework Programme (NanoEar, contract number: NMP4-CT-2006-026556), Academy of Finland (project number 115796), and Tampere Graduate Program in Biomedicine and Biotechnology (TGPBB). The authors thank Tommi Manninen and Weikai Zhang (University of Tampere) for plasmid propagation and extraction, Katri Paavilainen (Tampere University of Technology) for her assistance in nanoparticle preparation and characterization, and Ulla Kiiskinen (University of Tampere) for her excellent technical assistance.

References

Ahn, H. H., Lee, M. S., Cho, M. H., Shin, Y. N., Lee, J. H., Kim, K. S., et al. (2008). DNA/PEI nano-particles for gene delivery of rat bone marrow stem cells. *Colloids and Surfaces A: Physicochemical and Engineering Aspects*, *313-314*, 116–120.

Aktas, Y., Andrieux, K., Alonso, M. J., Calvo, P., Gürsoy, R. N., Couvreur, P., et al. (2005). Preparation and in vitro evaluation of chitosan nanoparticles containing a caspase inhibitor. *International Journal of Pharmaceutics*, *298*, 378–383.

Amidi, M., Romeijn, S. G., Borchard, G., Junginger, H. E., Hennink, W. E., & Jiskoot, W. (2006). Preparation and characterization of protein-loaded *N*-trimethyl chitosan nanoparticles as nasal delivery system. *Journal of Controlled Release*, *111*, 107–116.

Carlisle, R. C., Read, M. L., Wolfert, M. A., & Seymour, L. W. (1999). Self-assembling poly(L-lysine)/DNA complexes capable of integrin-mediated cellular uptake and gene expression. *Colloids and Surfaces B: Biointerfaces*, *16*, 261–272.

Chan, P., Kurisawa, M., Chung, J. E., & Yang, Y. Y. (2007). Synthesis and characterization of chitosan-g-poly(ethylene glycol)–folate as a non-viral carrier for tumor-targeted gene delivery. *Biomaterials*, *28*, 540–549.

Corsi, K., Chellat, F., Yahia, L., & Fernandes, J. C. (2003). Mesenchymal stem cells, MG63 and HEK293 transfection using chitosan–DNA nanoparticles. *Biomaterials*, *24*, 1255–1264.

Danielsen, S., Vårum, K. M., & Stokke, B. T. (2004). Structural analysis of chitosan mediated DNA condensation by AFM: Influence of chitosan molecular parameters. *Biomacromolecules*, *5*, 928–936.

Davis, M. E. (2002). Non-viral gene delivery systems. *Current Opinion in Biotechnology*, *13*, 128–131.

De Campos, A. M., Sánchez, A., & Alonso, M. J. (2001). Chitosan nanoparticles: A new vehicle for the improvement of the delivery of drugs to the ocular surface. Application to cyclosporin A. *International Journal of Pharmaceutics*, *224*, 159–168.

de la Fuente, M., Seijo, B., & Alonso, M. J. (2008). Novel hyaluronic acid–chitosan nanoparticles for ocular gene therapy. *Investigative Ophthalmology & Visual Science*, *49*, 2016–2024.

Dickerson, R. E., Drew, H. R., Conner, B. N., Wing, R. M., Fratini, A. V., & Kopka, M. L. (1982). The anatomy of A-, B-, and Z-DNA. *Science*, *216*, 475–485.

Erbacher, P., Zou, S., Bettinger, T., Steffan, A. M., & Remy, J. S. (1998). Chitosan-based vector/DNA complexes for gene delivery: Biophysical characteristics and transfection ability. *Pharmaceutical Research*, *15*, 1332–1339.

Gao, S., Chen, J., Xu, X., Ding, Z., Yang, Y. H., Hua, Z., et al. (2003). Galactosylated low molecular weight chitosan as DNA carrier for hepatocyte-targeting. *International Journal of Pharmaceutics*, *255*, 57–68.

García-Suárez, O., Hannestad, J., Esteban, I., Sainz, R., Naves, F. J., & Vega, J. A. (1998). Expression of the TrkB neurotrophin receptor by thymic macrophages. *Immunology*, *94*, 235–241.

Hashimoto, M., Morimoto, M., Saimoto, H., Shigemasa, Y., & Sato, T. (2006). Lactosylated chitosan for DNA delivery into hepatocytes: The effect of lactosylation on the physicochemical properties and intracellular trafficking of pDNA/chitosan complexes. *Bioconjugate Chemistry*, *17*, 309–316.

Hashimoto, M., Morimoto, M., Saimoto, H., Shigemasa, Y., Yanagie, H., Eriguchi, M., et al. (2006). Gene transfer by DNA/mannosylated chitosan complexes into mouse peritoneal macrophages. *Biotechnology Letters*, *28*, 815–821.

Hermanson, G. T. (1996). *Bioconjugate techniques* (1st ed.). San Diego, CA: Academic Press.

Huang, M., Fong, C. W., Khor, E., & Lim, L. Y. (2005). Transfection efficiency of chitosan vectors: Effect of polymer molecular weight and degree of deacetylation. *Journal of Controlled Release*, *106*, 391–406.

Jayakumar, R., Chennazhi, K. P., Muzzarelli, R. A. A., Tamura, H., Nair, S. V., & Selvamurugan, N. (2010). Chitosan conjugated DNA nanoparticles in gene therapy. *Carbohydrate Polymers*, *79*, 1–8.

Kiang, T., Wen, J., Lim, H. W., & Leong, K. W. (2004). The effect of the degree of chitosan deacetylation on the efficiency of gene transfection. *Biomaterials*, *25*, 5293–5301.

Kim, T. H., Park, I. K., Nah, J. W., Choi, Y. J., & Cho, C. S. (2004). Galactosylated chitosan/DNA nanoparticles prepared using water-soluble chitosan as a gene carrier. *Biomaterials*, *25*, 3783–3792.

Kim, T. H., Jin, H., Kim, H. W., Cho, M. H., & Cho, C. S. (2006). Mannosylated chitosan nanoparticle-based cytokine gene therapy suppressed cancer growth in BALB/c mice bearing CT-26 carcinoma cells. *Molecular Cancer Therapeutics*, *5*, 1723–1732.

Kunath, K., von Harpe, A., Fischer, D., Petersen, H., Bickel, U., Voigt, K., et al. (2003). Low-molecular-weight polyethylenimine as a non-viral vector for DNA delivery: Comparison of physicochemical properties, transfection efficiency and in vivo distribution with high-molecular-weight polyethylenimine. *Journal of Controlled Release*, *89*, 113–125.

Köping-Höggård, M., Mel'nikova, Y. S., Vårum, K. M., Lindman, B., & Artursson, P. (2003). Relationship between the physical shape and the efficiency of oligomeric chitosan as a gene delivery system *in vitro* and *in vivo*. *The Journal of Gene Medicine*, *5*, 130–141.

Lavertu, M., Méthot, S., Tran-Khanh, N., & Buschmann, M. D. (2006). High efficiency gene transfer using chitosan/DNA nanoparticles with specific combinations of molecular weight and degree of deacetylation. *Biomaterials*, *27*, 4815–4824.

Leong, K. W., Mao, H. Q., Truong-Le, V. L., Roy, K., Walsh, S. M., & August, J. T. (1998). DNA–polycation nanospheres as non-viral gene delivery vehicles. *Journal of Controlled Release*, *53*, 183–193.

Liu, W., Sun, S., Cao, Z., Zhang, X., Yao, K., Lu, W. W., et al. (2005). An investigation on the physicochemical properties of chitosan/DNA polyelectrolyte complexes. *Biomaterials*, *26*, 2705–2711.

Ma, Z., Wu, X., Cao, M., Pan, W., Zhu, F., Chen, J., et al. (2003). Selection of trkB-binding peptides from a phage-displayed random peptide library. *Science in China Series C Life Sciences*, *46*, 77–86.

MacLaughlin, F. C., Mumper, R. J., Wang, J., Tagliaferri, J. M., Gill, I., Hinchcliffe, M., et al. (1998). Chitosan and depolymerized chitosan oligomers as condensing carriers for in vivo plasmid delivery. *Journal of Controlled Release*, *56*, 259–272.

Mann, A., Richa, R., & Ganguli, M. (2008). DNA condensation by poly-L-lysine at the single molecule level: Role of DNA concentration and polymer length. *Journal of Controlled Release*, *125*, 252–262.

Mansouri, S., Cuie, Y., Winnik, F., Shi, Q., Lavigne, P., Benderdour, M., et al. (2006). Characterization of folate–chitosan–DNA nanoparticles for gene therapy. *Biomaterials*, *27*, 2060–2065.

Mao, H. Q., Roy, K., Troung-Le, V. L., Janes, K. A., Lin, K. Y., Wang, Y., et al. (2001). Chitosan–DNA nanoparticles as gene carriers: Synthesis, characterization and transfection efficiency. *Journal of Controlled Release*, *70*, 399–421.

Mattson, G., Conklin, E., Desai, S., Nielander, G., Savage, M. D., & Morgensen, S. (1993). A practical approach to crosslinking. *Molecular Biology Reports*, *17*, 167–183.

Muzzarelli, R. A. A. (2010). Chitins and chitosans as immunoadjuvants and non-allergenic drug carriers. *Marine Drugs*, *8*, 292–312.

Muzzarelli, R. A. A., Boudrant, J., Meyer, D., Manno, N., DeMarchis, M., & Paoletti, M. G. (2012). Current views of fungal chitin/chitosan, human chitinases, food preservation, glucans, pectins and inulin: A tribute to Henri Braconnot, precursor of the carbohydrate polymers science, on the chitin bicentennial. *Carbohydrate Polymers*, *87*, 995–1012.

Navarro, G., & Tros de ILarduya, C. (2009). Activated and non-activated PAMAM dendrimers for gene delivery in vitro and in vivo. *Nanomedicine: Nanotechnology, Biology, and Medicine*, *5*, 287–297.

Opanasopit, P., Rojanarata, T., Apirakaramwong, A., Ngawhirunpat, T., & Ruktanonchai, U. (2009). Nuclear localization signal peptides enhance transfection efficiency of chitosan/DNA complexes. *International Journal of Pharmaceutics*, *382*, 291–295.

Peng, S. F., Su, C. J., Wei, M. C., Chen, C. Y., Liao, Z. X., Lee, P. W., et al. (2010). Effects of the nanostructure of dendrimer/DNA complexes on their endocytosis and gene expression. *Biomaterials*, *31*, 5660–5670.

Richardson, S. C. W., Kolbe, H. V. J., & Duncan, R. (1999). Potential of low molecular mass chitosan as a DNA delivery system: Biocompatibility, body distribution and ability to complex and protect DNA. *International Journal of Pharmaceutics*, *178*, 231–243.

Romøren, K., Pedersen, S., Smistad, G., Evensen, Ø., & Thu, B. J. (2003). The influence of formulation variables on in vitro transfection efficiency and physicochemical properties of chitosan-based polyplexes. *International Journal of Pharmaceutics*, *261*, 115–127.

Strand, S. P., Lelu, S., Reitan, N. K., de Lange Davies, C., Artursson, P., & Vårum, K. M. (2010). Molecular design of chitosan gene delivery systems with an optimized balance between polyplex stability and polyplex unpacking. *Biomaterials*, *31*, 975–987.

Trapani, A., Lopedota, A., Franco, M., Cioffi, N., Ieva, E., Garcia-Fuentes, M., et al. (2010). A comparative study of chitosan and chitosan/cyclodextrin nanoparticles as potential carriers for the oral delivery of small peptides. *European Journal of Pharmaceutics and Biopharmaceutics*, *75*, 26–32.

van der Lubben, I. M., Verhoef, J. C., van Aelst, A. C., Borchard, G., & Junginger, H. E. (2001). Chitosan microparticles for oral vaccination: Preparation, characterization and preliminary in vivo uptake studies in murine Peyer's patches. *Biomaterials*, *22*, 687–694.

Wightman, L., Kircheis, R., Rössler, V., Carotta, S., Ruzicka, R., Kursa, M., et al. (2001). Different behavior of branched and linear polyethylenimine for gene delivery *in vitro* and *in vivo*. *The Journal of Gene Medicine*, *3*, 362–372.

Xu, X., Capito, R. M., & Spector, M. (2008). Plasmid size influences chitosan nanoparticle mediated gene transfer to chondrocytes. *Journal of Biomedical Materials Research*, *84A*, 1038–1048.

Yuan, X. B., Li, H., & Yuan, Y. B. (2006). Preparation of cholesterol-modified chitosan self-aggregated nanoparticles for delivery of drugs to ocular surface. *Carbohydrate Polymers*, *65*, 337–345.

Zheng, F., Shi, X. W., Yang, G. F., Gong, L. L., Yuan, H. Y., Cui, Y. J., et al. (2007). Chitosan nanoparticle as gene therapy vector via gastrointestinal mucosa administration: Results of an in vitro and in vivo study. *Life Sciences*, *80*, 388–396.